Tiled-aperture coherent beam combining of two high-power fibre amplifiers

Zhou Pu(周 朴), Ma Yan-Xing(马阎星), Wang Xiao-Lin(王小林),
Ma Hao-Tong(马浩统), Xu Xiao-Jun(许晓军), and Liu Ze-Jin(刘泽金)†

College of Optoelectric Science and Engineering, National University of Defense Technology, Changsha 410073, *China*

(Received 8 June 2009; revised manuscript received 25 June 2009)

We demonstrate coherent beam combining of two tiled-aperture single-frequency fibre amplifiers with a total output power of 29.65 W by using the multi-dithering technique. The two laser beams are packaged closely by using free-space mirrors side by side into a tiled-aperture with a near-field fill factor of 62%. Active phase control of the amplifier is performed on commercially available digital lock-in amplifiers. Experimental results show that the power contained in the main-lobe in closed-loop is 1.72 times greater than that in open-loop, which is 86% for the ideal case. The fringe contrast of the far-field fringe pattern is as high as 80% when the system is in closed-loop. The beam quality of the combined beam is computed to be BQ = 1.48. The whole system in closed-loop performs well in a long-time observation.

Keywords: coherent beam combination, multi-dithering, tiled-aperture

PACC: 4225K, 4255N, 4260F

1. Introduction

Coherent beam combining of fibre lasers/amplifiers was intensively researched recently.[1−13] As a promising approach, coherent beam combining based on the multi-dithering technique is of great potential in scaling to a large number of beamlets and free of reference beams.[9−13] With this technique, Shay *et al.*[10] combined coherently up to nine-channel fibre amplifiers. In the previous demonstrations, the beam quality of the coherently combined beamlets was degraded due to the small fill-factor of the laser array and much of the laser power was distributed in the multiple side-lobes.[10−13] In addition, specially designed signal processing blocks for phase modulation at a radio frequency (RF) as high as more than 100 MHz were employed in the previous demonstrations, which made a significant increase in system cost. We have successfully demonstrated a coherent beam combination of watt-level fibre amplifiers with commercially available digital lock-in amplifiers.[13] Nevertheless, the bandwidth of phase fluctuation becomes high as amplifier output power increases. In the present paper, we further study our experimental investigation on enhancing coherent beam combining of fibre amplifiers using the multi-dithering technique and commercially available digital lock-in amplifiers to a higher output power. The whole experimental system is of a tiled-aperture configuration, which brings a significant improvement in the fill-factor of the laser array and the beam quality of the coherently combined beam in the receiving plane.

2. Theory of the multi-dithering technique

A typical schematic diagram of coherent beam combining with the multi-dithering technique is shown in Fig. 1. A single frequency master laser is split into two channels, each with a fibre amplifier module to enhance the laser power to a higher level. Channel B is phase-modulated by a signal generator.

The complex fields of the two channels can be written as

$$E_{\rm A}(t) = E_{\rm AO}\cos(\omega_{\rm L}t + \phi_{\rm A})\ , \tag{1}$$

$$E_{\rm B}(t) = E_{\rm BO}\cos(\omega_{\rm L}t + \phi_{\rm B} + \beta_{\rm m}\sin(\omega_{\rm m}t))\ , \tag{2}$$

where $E_{\rm AO}$ and $E_{\rm BO}$ represent the field amplitudes, $\phi_{\rm A}$ and $\phi_{\rm B}$ refer to the optical phases, $\beta_{\rm m}$ and $\omega_{\rm m}$ are the amplitude and the frequency of the phase modulation signal added to channel B, respectively, and $\omega_{\rm L}$ denotes the laser frequency.

†Corresponding author. E-mail: zejinliu@vip.sina.com

© 2010 Chinese Physical Society and IOP Publishing Ltd

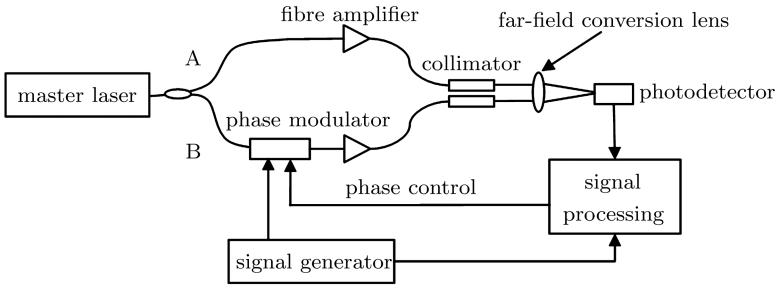


Fig. 1. Schematic diagram of the multi-dithering technique principle.

The optical fields from channels A and B are overlapped on the photodetector. The optical intensity at the centre of the photodetector can be expressed as

$$\begin{aligned} I(t) &= [E_{\rm A}(t) + E_{\rm B}(t)]^2 \\ &= E_{\rm A}^2(t) + E_{\rm B}^2(t) + 2E_{\rm A}(t)E_{\rm B}(t). \end{aligned} \tag{3}$$

The following expression can be obtained by using the trigonometric identity of the product of two cosines:

$$\begin{aligned} & 2E_{\rm A}(t)E_{\rm B}(t) \\ &= E_{\rm AO}E_{\rm BO}\{\cos[2\omega_{\rm L} + \phi_{\rm A} + \phi_{\rm B} + \beta_{\rm m}\sin(\omega_{\rm m}t)] \\ &\quad + \cos[\phi_{\rm B} - \phi_{\rm A} + \beta_{\rm m}\sin(\omega_{\rm m}t)]\}. \end{aligned} \tag{4}$$

Neglecting the term oscillating at optical frequencies and substituting the trigonometric identity for the cosine of the sum of two angles and the Fourier series expansions for cosine and sine of $\beta_{\rm m}\sin(\omega_{\rm m}t)$, we can obtain

$$\begin{aligned} & E_{\rm AO}E_{\rm BO}\cos[\phi_{\rm B} - \phi_{\rm A} + \beta_{\rm m}\sin(\omega_{\rm m}t)] \\ &= E_{\rm AO}E_{\rm BO}\{\cos(\phi_{\rm B} - \phi_{\rm A})[{\rm J}_0(\beta_{\rm m}) \\ &\quad + 2({\rm J}_2(\beta_{\rm m})\cos(2\,\omega_{\rm m}t) + {\rm J}_4(\beta_{\rm m})\cos(4\omega_{\rm m}t) + \ldots)] \\ &\quad - 2\sin(\phi_{\rm B} - \phi_{\rm A})[{\rm J}_1(\beta_{\rm m})\sin\omega_{\rm m}t \\ &\quad + {\rm J}_3(\beta_{\rm m})\sin(3\,\omega_{\rm m}t) + \cdots]\}, \end{aligned} \tag{5}$$

where J represents a Bessel function of the first kind. The output photocurrent of photodetector can be expressed as

$$i_{\rm PD}(t) = R_{\rm PD}SI(t), \tag{6}$$

where $R_{\rm PD}$ represents the responsivity of the photodetector, and S denotes the photodetector area. The phase control signal is extracted from the photocurrent by using coherent demodulation. The photodetector current is multiplied by $\sin(\omega_{\rm m}t)$ and integrated over time τ. The integration time$\tau$is selected to be long enough to isolate the individual phase control signals of the phase-modulated elements and short enough for the phase control loop to effectively cancel the phase disturbances. The control signal for Channel B is thus given by[10−12]

$$\begin{aligned} V_{\rm S} &= \frac{1}{\tau}\int_0^{\tau} i_{\rm PD}\sin(\omega_{\rm m}t)\,{\rm d}t \\ &\approx R_{\rm PD}SE_{\rm AO}E_{\rm BO}{\rm J}_1(\beta_{\rm m})\sin(\phi_{\rm A} - \phi_{\rm B}). \end{aligned} \tag{7}$$

3. Experimental setup and results

The experimental setup is shown in Fig. 2. The master oscillator is a pigtailed Nd: YVO_4 linear polarized single-frequency laser with a 1064 nm central wavelength and a linewidth less than 1 MHz. The laser beam is pre-amplified (PA1) before its splitting into eight channels and then coupled to phase modulators (PM). In our present experiment only two channels are employed. The phase modulators are home-made by entwining a 10-metre-long polarization-maintained fibre around a cylindrical piezoelectric ceramic transducer (PZT) with a diametre of 2 cm. The laser beams from the phase modulators are then sent to a second pre-amplifier (PA2), the main amplifier (MA) and an optical isolator (ISO) and into two specially desiged large-diametre collimators. The diametre of laser beam output from the collimator is 6 mm. The laser beams are tiled closely by using free-space mirrors side by side into a tiled-aperture so that they behave as one single coherent beam. The fill factor is defined as the beam diametre divided by the distance of the adjacent beamlets. The fill factor of the near-field laser array is calculated to be 62%. The tilt angles of the laser beams are carefully tuned to ensure that the two laser beams overlap with each other in

the receiving plane after passing through a 10-metre propagation distance. The simulated turbulence is induced by the round-the-clock working of the cooling fans fixed on the ceiling of the room. The two collimated output beams are sampled by a mirror. After the splitter, part of the beam is sent into a pinhole with a 95 μm radius, a photoelectric detector is located immediately behind the pinhole. The location of the pinhole is adjusted by opening one of the laser channels to obtain the maximum output signal of the detector. Then the pinhole location is fixed, the other laser channel kept open, and the collimator adjusted so as to find the maximum output signal of the detector. In this way, the central portion of the main-lobe can be imaged into the detector after the signal passes through the pinhole.

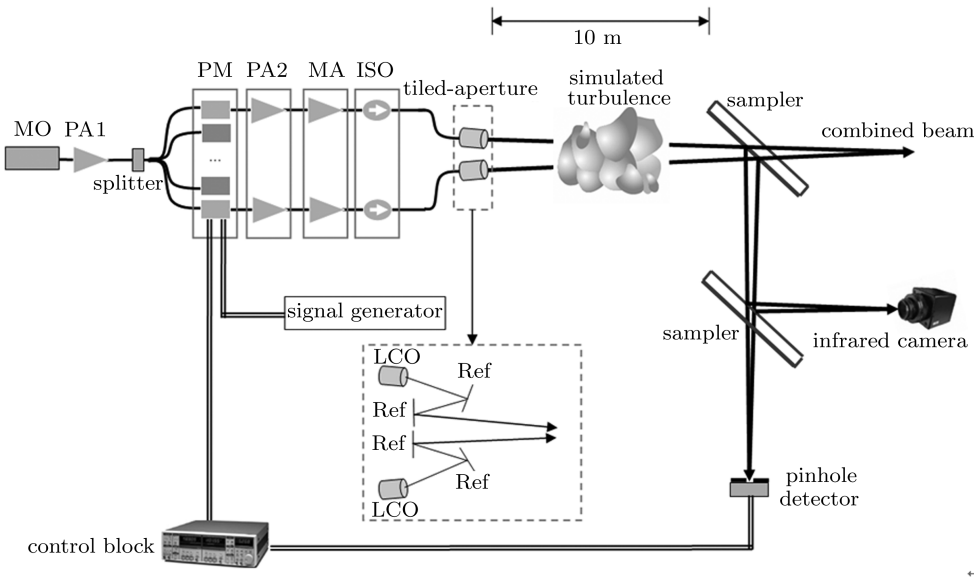


Fig. 2. Experimental setup (MO: master oscillator. PA: pre-amplifier. PM: phase modulator. MA: main amplifier. ISO: optical isolator. LCO: large diametre collimator. Ref: reflector.).

The main amplifier comprises two 5-metre-long double-clad polarization-maintained Yb-doped fibres. In the experiment, the main amplifier is end-pumped by a maximal 25 W laser diode with a peak intensity emission at 975 nm at 40 A pump current. Aspheric lenses are designed for coupling the pump beams into the inner cladding of the double-clad fibre. All the fibre ends are cleaved at an angle of $\sim$8 ℃ to suppress parasitic oscillations. By careful adjustment it is possible to couple more than 200 mW master emission from the second pre-amplifier into the double-clad active fibre, in which the fundamental mode can almost entirely propagate. The output power characteristics of the main amplifiers are shown in Fig. 3. The maximum output powers of the two amplifiers are 15.4 W and 14.25 W, separately. The total output power of the two amplifiers is about 29.65 W.

Coherent beam combining is realized by active phase control using the multi-dithering technique. The

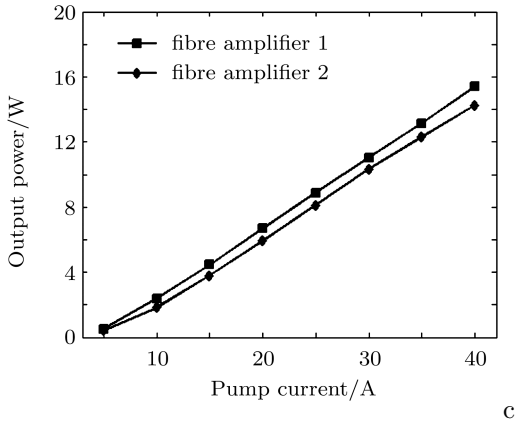


Fig. 3. Output power characteristics of two main fibre amplifiers.

phase control signal is generated according to expression (7), which can be implemented by commercial SR830 digital lock-in amplifiers produced by Stanford

Research Systems[13] in our experiment. In the experiment, when the two amplifiers are both turned on, the whole system is in open-loop and the phase control based on the multi-dithering technique is not implemented, the far-field fringe is blurred and shifts fast due to fast phase fluctuation in each fibre amplifier. An image of the far-field intensity distribution is shown in Fig. 4(a), which indicates a result of incoherent beam combining.

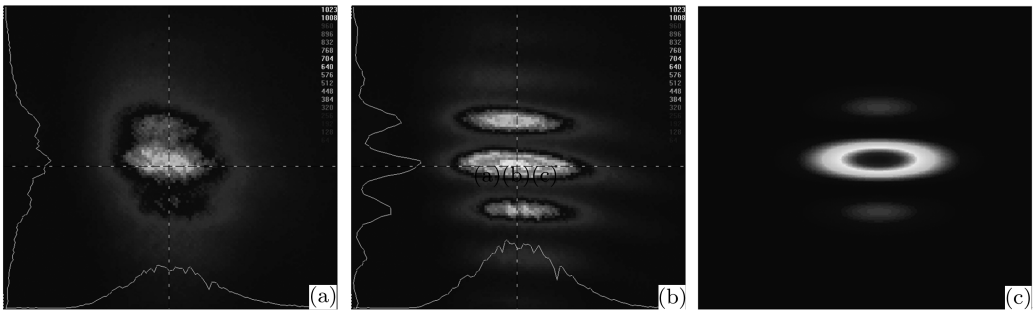


Fig. 4. Intensity profiles in the observing plane, where panel (a) shows experimental beam profiles in open-loop, panel (b) shows experimental beam profiles in closed-loop, and panel (c) displays simulated beam profiles in closed-loop.

In the closed-loop endeavours, the frequency and the amplitude of the modulation signal are chosen to be 60 kHz and 80 mV, respectively, and the integration time of the lock-in amplifier is set to be 100 μs. The far-field fringe is clear and steady and an image of the far-field intensity distribution is shown in Fig. 4(b). The contrast of the coherently combined beam profile is calculated to be more than 80%, where the fringe contrast is determined from the formula $(I_{\max} - I_{\min})/(I_{\max} + I_{\min})$, where $I_{\max}$ and $I_{\min}$ are the maximum optical intensity and the adjacent minimum on the intensity pattern, respectively. The power contained in the central main-lobe is enhanced by a factor of 1.72, which is 86% of that for the ideal coherently combining case (in the ideal case the power contained in the central main-lobe was enhanced by a factor of 2). As a reference for evaluating the beam profile in the closed-loop, the theoretical far-field pattern is computed and presented in Fig. 4(c). It is found that the experimental result is in agreement with the theoretical one. The power contained in the main-lobe can be obtained by digital image processing of the beam profile grabbed by the camera, i.e. the summation of the pixel values in the specified bucket denoting the main-lobe, divided by all the pixel values in the whole image. The power contained in the main lobe in Fig. 4(b) is computed to be 38.3%. In the previously published literature, the power contained in the main-lobe was less than 10% of that estimated from the far-field intensity patterns. It can be concluded that the power contained in the central main-lobe is well improved compared with previous demonstrations[10−13] due to the tiled-aperture output configuration. The beam quality of the combined beam, BQ, is calculated to be 1.48, i.e. BQ = 1.48, where the beam quality is computed from the formula[3] BQ $= (P/P_{\rm DL})^{-1/2}$, where P and $P_{\rm DL}$ are the powers contained within a bucket of radius λ/D for the measured beam and a diffraction-limited beam with the same near-field full width D, respectively. The whole system in closed-loop performs well in a long-time observation.

4. Conclusions

In this paper, we experimentally investigate the enhancement of coherent beam combining of fibre amplifiers by using the multi-dithering technique and commercially available digital lock-in amplifiers to a total output power of 29.65 W. Experimental results show that the power contained in the main-lobe in closed-loop is 1.72 times greater than that in open-loop, which is 86% of that for the ideal case. The two laser beams are located side-by-side to form a tiled-aperture, which makes a significant improvement in the beam quality of the combined beam. The beam quality of the coherently combined beam, BQ, is 1.48,

i.e. BQ = 1.48, and the contrast of the coherently combined beam profile is as high as 80% when the system is in closed-loop. The phase fluctuating frequency of a large-mode-area ytterbium-doped fibre amplifier at 260 W output power in a relatively quiet lab environment is well below several hundred Hz.[14] Considering the fact that the modulation frequency of the commercial digital lock-in amplifier can be tuned to be more than 100 kHz, which presents sufficient control bandwidth for the multi-hundred watt level fibre amplifiers, it is believed that coherent beam combination of fibre amplifiers by using the multi-dithering technique and commercially available digital lock-in amplifiers still has the potential to achieve a much higher output power.

References

[1] Anderegg J, Brosnan S, Cheung E, Epp P, Hammons D, Komine H, Weber M and Wickham M 2006 *Proc. SPIE.* **6102** 61020U-1

[2] Augst S J, Ranka J K, Fan T Y and Sanchez A 2007 *J. Opt. Soc. Am.* B **24** 1707

[3] Goodno G D, Asman C P, Anderegg J, Brosnan S, Cheung E C, Hammons D, Injeyan H, Komine H, Long W H, Jr., McClellan M, McNaught S J, Redmond S, Simpson R, Sollee J, Weber M, Weiss S B and Wickham M 2007 *IEEE J. Sel. Top. Quantum Electron.* **13** 460

[4] Xiao R, Hou J and Jiang Z F 2006 *Acta Phys. Sin.* **55** 6464 (in Chinese)

[5] Wang J M, Duan K L and Wang Y S 2008 *Acta Phys. Sin.* **57** 5627 (in Chinese)

[6] Peng Q, Zhou Y, Chen Y, Sun Z, Bo Y, Yang X, Xu Z, Wang Y, Li K and Zhao W 2005 *Electron. Lett.* **41** 171

[7] Jia X J, Liu F N, Fu S G, Liu Y G, Yuan S G and Dong X Y 2007 *Chin. Phys* **16** 2993

[8] He B, Lou Q H, Wang W, Zhou J, Zheng Y H, Dong J X, Wei Y R and Chen W B 2008 *Appl. Phys. Lett.* **92** 251115

[9] Liu L, Loizos D N, Vorontsov M A, Sotiriadis P P and Cauwenberghs G 2007 *Proc. SPIE.* **6708** 67080D-1

[10] Shay T M, Benham V, Baker J T, Sanchez A D, Pilkington D and Lu C A 2007 *IEEE J. Sel. Top. Quantum Electron.* **13** 480

[11] Shay T M, Benham V, Baker J T, Ward B, Sanchez A D, Culpepper M A, Pilkington D, Spring J, Nelson D and Lu C A 2006 *Opt. Express* **14** 12022

[12] Shay T M, Baker J T, Sanchez A D, Robin C A, Vergien L C L, Zerinque C, Gallant D, Lu C A, Pulford B, Bronder T J and Lucero A 2009 *Proc. SPIE.* **7195** 71951M-1

[13] Ma Y X, Liu Z J, Zhou P, Wang X L, Ma H T, Li X, Xu X J and Si L 2009 *Chin. Phys. Lett.* **26** 044204

[14] Jones D C, Stacey C D and Scott A M 2007 *Opt. Lett.* **32** 466